Available online at www.sciencedirect.com

SCIENCE DIRECT®

Earth and Planetary Science Letters 223 (2004) 35–48

EPSL

www.elsevier.com/locate/epsl

The thermal effects of steady-state slab-driven mantle flow above a subducting plate: the Cascadia subduction zone and backarc

C.A. Currie[a,b,*], K. Wang[a,b,1], Roy D. Hyndman[a,b,2], Jiangheng He[b,3]

[a] *School of Earth and Ocean Sciences, University of Victoria, P.O. Box 3055, Victoria, BC, Canada V8W 3P6*
[b] *Pacific Geoscience Centre, Geological Survey of Canada, P.O. Box 6000, Sidney, BC, Canada V8L 4B2*

Received 24 November 2003; received in revised form 8 April 2004; accepted 16 April 2004

Abstract

At subduction zones, geophysical and geochemical observations indicate that the arc and backarc regions are hot, in spite of the cooling effects of a subducting plate. At the well-studied Cascadia subduction zone, high mantle temperatures persist for over 500 km into the backarc, with little lateral variation. These high temperatures are even more surprising due to the juxtaposition of the hot Cascadia backarc against the thick, cold North America craton lithosphere. Given that local heat sources appear to be negligible, mantle flow is required to transport heat into the wedge and backarc. We have examined the thermal effects of mantle flow induced by traction along the top of the subducting plate. Through systematic tests of the backarc model boundary, we have shown that the model thermal structure of the wedge is primarily determined by the assumed temperatures along this boundary. To get high temperatures in the wedge, it is necessary for flow to mine heat from depth, either by using a temperature-dependent rheology, or by introducing a deep cold boundary through a thick adjacent lithosphere, consistent with the presence of a craton. Regardless of the thermal conditions along the backarc boundary, flow within an isoviscous wedge is too slow to transport a significant amount of heat into the wedge corner. With a more realistic stress- and temperature-dependent wedge rheology, flow is focused into the wedge corner, resulting in rapid flow upward toward the corner and enhanced temperatures below the arc, compatible with temperatures required for arc magma generation. However, this strong flow focusing produces a nearly stagnant region further landward in the shallow backarc mantle, where model temperatures and heat flow are much lower than observed. Observations of high backarc temperatures, particularly in areas that have not undergone recent extension, provide an important constraint on wedge dynamics. None of the models of simple traction-driven flow were able to simultaneously produce high temperatures beneath the volcanic arc and throughout the backarc. The most likely way to produce hot and isothermal conditions in the backarc is through vigorous small-scale-free convection in a low-viscosity asthenosphere.

Keywords: Subduction zones; Cascadia; Mantle wedge; Backarc; Thermal structure; Mantle flow; Numerical modelling; Corner flow

* Corresponding author. Pacific Geoscience Centre, Geological Survey of Canada, P.O. Box 6000, 9860 West Saanich Road, Sidney, BC, Canada V8L 4B2. Tel.: +1-250-363-6844; fax: +1-250-363-6565.

E-mail addresses: ccurrie@nrcan.gc.ca (C.A. Currie), kwang@nrcan.gc.ca (K. Wang), rhyndman@nrcan.gc.ca (R.D. Hyndman), he@pgc.nrcan.gc.ca (J. He).

[1] Tel.: +1-250-363-6429.

[2] Tel.: +1-250-363-6428.

[3] Tel.: +1-250-363-6441.

0012-821X/$ - see front matter.
doi:10.1016/j.epsl.2004.04.020

1. Introduction

A remarkable feature of subduction zones is that the mantle beneath the volcanic arc and well into the backarc is hot, even in areas that have not undergone recent extension. Indeed, to produce arc magmas, geochemical analyses suggest that temperatures >1200 °C are required in the mantle wedge [1,2]. The observed high temperatures are contradictory to the expected cooling effects of a subducting plate, which represents a substantial heat sink. Many studies have concluded that local sources of heat, such as frictional heating along the subducting plate surface, heat associated with metamorphism, and radiogenic heat production, are insufficient to produce the observed high temperatures [3–7]. Thus, mantle flow is invoked as a mechanism for transporting heat into the mantle wedge [8–10]. Such flow can be driven by traction between the downgoing plate and mantle wedge (forced convection) or thermal buoyancy (free convection) (Fig. 1).

The majority of numerical modelling studies have primarily focussed on traction-driven flow [2,11–17]. With traction-driven flow, mantle wedge material immediately above the slab is entrained and carried downward with the slab. This material is then replaced by hot material from the backarc. Previous studies have shown that this flow has a significant effect on mantle temperatures below the arc, as well as temperatures within the subducting slab.

The interpretation of the thermal models requires an understanding of the influence of boundary conditions and model parameters. It is clear that the thermal structure of the incoming oceanic plate strongly affects temperatures in the forearc region, as well as temperatures in the interior of the slab [7,15,16,18]. In this study, we assess the importance of the thermal boundary conditions along the backarc (landward) boundary of the models. In the models below, as in many previous studies, material enters the wedge through this boundary. As we show, the resulting thermal structure in the wedge is strongly affected by the boundary location, as well as the prescribed temperatures along this boundary.

We then look at the heat budget at a subduction zone and examine how traction-driven mantle wedge flow distributes heat, using either an isoviscous or stress- and temperature-dependent mantle rheology. The thermal models may be compared with observational constraints to evaluate the validity of traction-

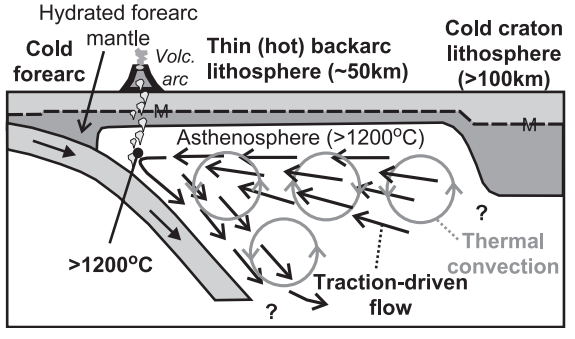

Fig. 1. Schematic diagram of the geometry and key temperature constraints for the northern Cascadia subduction zone. Two wedge flow geometries are also shown: traction-driven corner flow and thermal convection.

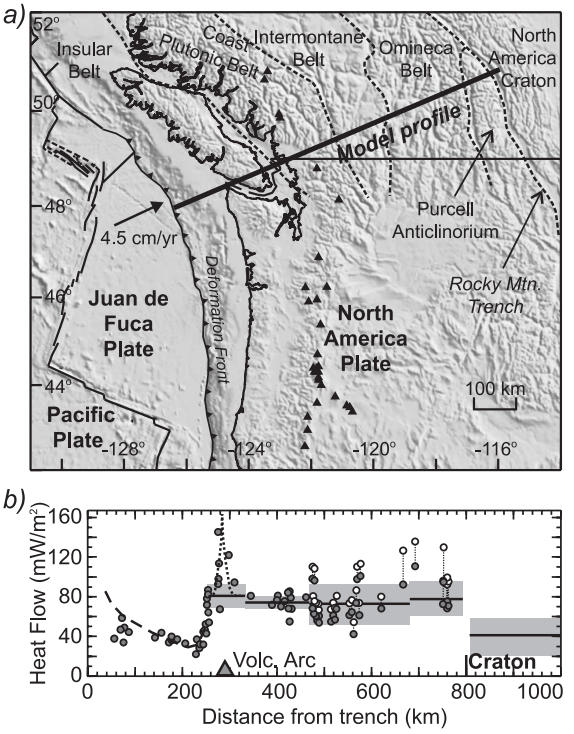

Fig. 2. (a) Map of the Cascadia subduction zone with the profile location for the 2D models. (b) Heat flow measurements within 150 km of the profile [19,20,26,29]. The observed heat flow values (open circles) and averages (with standard deviation bounds) have been corrected for the eastward increase in crustal heat generation (solid circles).

driven flow for bringing heat into the mantle wedge and backarc. A number of observations indicate that backarcs are hot for hundreds of kilometres behind the volcanic arc. We argue that this is a critical constraint for wedge flow models.

We focus our study on the northern Cascadia subduction zone (48–51°N) where the thermal structure is well constrained and where no significant recent backarc extension has occurred (Fig. 2). Although there was short-lived (<10 myr) Eocene extension in a small area in the easternmost backarc (49–50°N; eastern Omineca Belt) [19–21], there is no evidence for late Cenozoic extension [21]. The Cascadia backarc is limited on its eastern boundary by the North America craton. Cratons are noted for their low surface heat flow (~ 42 mW/m^2) and low mantle heat flow (10–20 mW/m^2), and high seismic velocity anomalies that extend several hundred kilometres down into the mantle (e.g., [22–25]), indicating cool temperatures to great depths. The presence of the adjacent cold craton makes high backarc temperatures even more surprising.

2. Observational constraints

One of the key constraints on deep subduction zone thermal structure is surface heat flow. Over the Cascadia forearc, surface heat flow is low (30–40 mW/m^2) due to the cooling effect of the subducting slab [26–28] (Fig. 2). Approximately 30 km seaward of the volcanic arc, surface heat flow increases to over 80 mW/m^2. Near the volcanic centres, there is considerable scatter in the heat flow values, which likely reflects local processes such as magma emplacement and groundwater flow [29,30]. Away from the volcanic centres, the background heat flow along the arc is ~ 80 mW/m^2 [27–29], consistent with petrological and seismic constraints that indicate temperatures >1200 °C in the shallow (40–70 km) mantle below the arc [2,31]. We focus on regional heat flow, excluding the local extreme values associated with volcanism.

For Cascadia, it is well established that high mantle temperatures are not localized at the volcanic arc. Heat flow remains high well into the backarc regions for the entire Cascadia subduction zone. In southern British Columbia, surface heat flow increases from ~ 75 mW/m^2 in the Intermontane Belt to over 100 mW/m^2 in the eastern Omineca Belt [20,29]. The eastward increase in surface heat flow appears to be the result of an increase in crustal radiogenic heat production from ~ 1 μW/m^3 in the Intermontane Belt to more than 3 μW/m^3 in the eastern Omenica Belt, such that the deep heat flow is similar [19,29]. In Washington and Oregon, a similar backarc heat flow of 75–90 mW/m^2 is observed, with local variations attributed to varying crustal heat production [27,28]. The reduced (deep crust/mantle) heat flow for all regions is 55–65 mW/m^2 [19,27,28], suggesting that there is little variation in the deep thermal structure for the entire Cascadia backarc. One-dimensional geotherms based on local heat generation give temperatures of 800–900 °C for the Moho (35 km depth) and ~ 1200 °C for the base of the backarc lithosphere (50–60 km depth) [19]. In the models below, we have used a uniform radiogenic heat production of 1.3 μW/m^3 in a 10-km-thick upper crust. To facilitate comparison of the models with the observed heat flow, each heat flow measurement was adjusted to the model heat production rate over a 10-km-thick upper crust (Fig. 2). After this adjustment, the surface heat flow for the northern Cascadia backarc is quite constant (75 ± 15 mW/m^2).

The landward limit of the hot Cascadia backarc in SW Canada is concluded to coincide with the Rocky Mountain Trench, 500 km east of the volcanic arc, based on rapid changes in surface heat flow, Pn velocity, and crustal thickness [19]. This area marks the eastern edge of the stable North America craton. The average heat flow over the Archean North America craton is 42 ± 10 mW/m^2 [23,24], implying much cooler deep temperatures relative to the adjacent backarc. Temperatures at the Moho (45–50 km depth) are estimated to be only 400–500 °C [19].

An initial compilation of thermal data from other backarcs suggests that they are similarly hot. High and nearly constant heat flow of 80–100 mW/m^2 is observed for over 400 km across the backarc of the Central Andean subduction zone (~ 21°S) [32]. Although the overlying continental crust is 60–70 km thick in this region, crustal heat production accounts for only 20–40 mW/m^2 [33]. Surface heat flow measurements for the backarcs of western Pacific subduction zones are generally high (>60 mW/m^2) [34]. In some of these regions, the high heat flow is, in

part, due to recent extension. However, for older basins, the average surface heat flow is 80–90 mW/m^2, regardless of basin age, suggesting that the backarc arc mantle is extremely hot due to another process. Further examination of global backarc temperature indicators is required to fully constrain the thermal structure of the mantle wedge in general.

3. Model description

3.1. Model geometry and boundary conditions

Steady-state finite element numerical models are used to investigate the thermal effects of traction-driven wedge flow, with the northern Cascadia subduction zone as the main example. In the two-dimensional models, a kinematically prescribed subducting slab drives flow within the viscous mantle wedge (Fig. 3). Thermal buoyancy is not included in the models. The geometry of the subducting plate to ~ 60 km depth has been constrained by seismic data and Wadati–Benioff seismicity [35]. At greater depths, teleseismic studies suggest that the plate dip increases to ~ 60° [36]. The thickness of the overriding crust is 35 km throughout the forearc and backarc regions [37,38]. The base of the rigid lithosphere is at 50 km depth, consistent with the depth of the lithosphere–asthenosphere boundary inferred from shear structures in mantle xenoliths from this region [39] and from thermal estimates [19]. The landward (eastern) boundary of

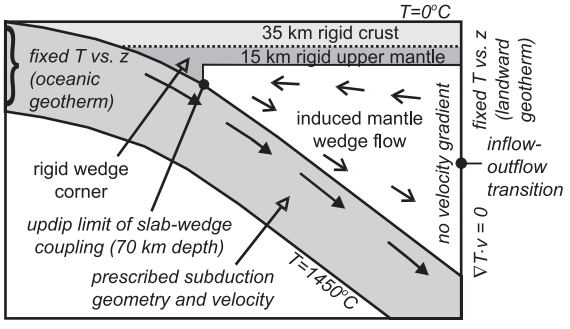

Fig. 3. Schematic model geometry and boundary conditions for the 2D subduction zone models. Flow in the wedge is driven by full coupling between the subducting slab and overlying mantle below 70 km depth. Flow is only calculated in the white region of the wedge.

the models is 800 km from the trench, in agreement with the inferred landward extent of the backarc and western limit of the North America craton.

Flow within the viscous wedge is calculated for an incompressible Boussinesq fluid (e.g., [16]). Previous studies have shown that the rheology of the wedge exerts a strong control on the flow structure (e.g., [13,16]). We have investigated models with a constant wedge viscosity and a temperature- and stress-dependent (nonlinear) viscosity, using the power law rheology for dislocation creep of wet olivine [40], based on the assumption that there is substantial input of water to the wedge from dehydration of the underlying subducting slab. The upper boundary of the wedge is assumed to be fully coupled to the stationary overriding plate. The part of the wedge in contact with the slab is dragged downward at the subduction rate. We use a subduction rate of 4.5 cm/year, consistent with estimates for northern Cascadia [41]. We allow flow through the landward boundary of the model below the lithosphere, using a boundary condition which requires that there be no velocity gradient across the boundary.

Wedge flow is prohibited from entering the wedge tip by placing a vertical boundary in the wedge where the subducting plate is at a depth of 70 km. Seaward of this boundary, the wedge is assumed to be rigid. The observed forearc heat flow is consistent with cooling of the forearc by the subducting plate [18,42], indicating that wedge flow does not extend into the tip of the wedge. Based on a similar heat flow profile for the NE Japan subduction zone, Furukawa [13] suggested that the slab and wedge are decoupled to depths of ~ 70 km by high pore pressure along the slab surface. Alternatively, hydration and serpentinization of the forearc mantle wedge could provide a mechanism for isolating the corner from wedge flow [43,44].

The steady-state heat equation is used to calculate the temperature within the entire model space. Real temperature is used throughout the calculations. Results are similar if potential (zero pressure) temperature is used, with a conversion to real temperature for output. The only local heat source included in the models is radioactive heating. Other local heat sources are assumed to be negligible (see discussion below). The entire model crust has a thermal conductivity of 2.5 W/mK, with radiogenic heat production of 1.3

$\mu W/m^3$ in the upper 10 km and 0.4 $\mu W/m^3$ in the lower 25 km. The mantle and subducting plate both have a thermal conductivity of 3.1 W/mK and radiogenic heat production of 0.02 $\mu W/m^3$, similar to that inferred from mantle xenoliths [23]. Reasonable variations in the thermal parameters have only a minor effect on the model results. Variations in crustal heat production, including a landward increase consistent with Cascadia backarc observations, have a direct effect on the surface heat flow, but only a negligible effect on wedge temperatures (<15 °C). We have also tested a temperature-dependent thermal conductivity [45]. For both an isoviscous and nonlinear rheology, the temperature-dependent conductivity leads to wedge temperatures that are ~ 12 °C lower than models with a constant thermal conductivity.

The upper boundary of the model has a constant temperature of 0 °C. The base of the model is the inclined bottom of the subducting slab, taken to be 95 km below the slab surface. A constant temperature of 1450 °C is assigned to this boundary. Uncertainties in this temperature have a negligible effect on the upper part of the subducting slab and mantle wedge due to the efficient advective heat transfer from the oceanic boundary by the subducting slab. A geotherm is prescribed to the oceanic boundary consistent with a 8-Ma oceanic plate overlain by 3 km of sediments [46,47].

Although we use the Cascadia subduction parameters, the primary objective of this study is to examine the effects of the landward boundary on the thermal structure of the wedge in general. Because flow passes through this boundary, the assumed thermal boundary conditions determine the temperature of material entering the mantle wedge. Three different geotherms have been tested (Fig. 4): (1) a "cool" geotherm that gives a surface heat flow of 42 mW/m^2, typical of cratons [23,24]; (2) a "warm" geotherm with a surface heat flow of 75 mW/m^2, consistent with the Cascadia backarc [19]; and (3) a "hot" geotherm producing a surface flow of 90 mW/m^2, representative of an extremely hot backarc. Each geotherm was calculated by assuming a conductive gradient, based on the surface heat flow and the thermal properties of the model crust and mantle. At depths greater than the intersection of the conductive geotherm with the mantle adiabat, an adiabatic gradient of 0.3 °C/km was used. The mantle adiabat corresponds to a mantle potential temperature of 1295 °C, consistent with experimental constraints on the temperature of the 410-km phase transition [48]. Temperatures are prescribed along the landward boundary of the overriding plate and the inflow part of the wedge. Along the outflow boundary, we assume no conductive heat flux parallel to flow lines across the boundary. The position of the inflow/outflow transition point depends on the wedge rheology and subducting plate geometry. This point is iteratively determined by the modelling code.

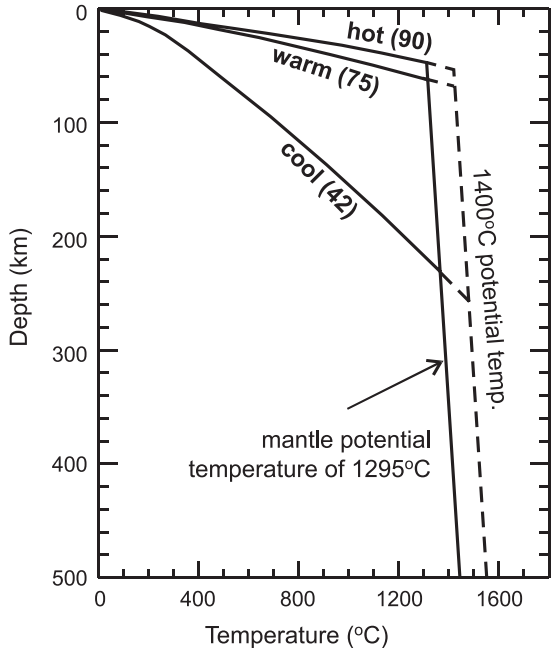

Fig. 4. Geotherms prescribed to the landward (backarc) boundary. The numbers in brackets indicate the surface heat flow for each geotherm (mW/m^2). The transition from a conductive gradient to an adiabatic gradient (0.3 °C/km) is determined by the mantle potential (zero pressure) temperature of 1295 °C (solid lines) or 1400 °C (dashed lines).

3.2. Numerical methods

The numerical models use nine-node isoparametric elements for the temperature and velocity fields and compatible four-node elements for the pressure field. The Cascadia models have 4802 elements, with element sizes ranging from 0.1 to 30 km, giving an average element size of 9 km. The nine-node quadrat-

ic elements allow high spatial resolution with relatively large elements. Note that resolution in finite element calculations is not determined solely by element size. With quadratic elements, resolution can be improved by a factor of 10 or more compared to linear elements of the same size.

In more detail, our modeling approach uses the conventional penalty function formulation to stabilize pressure solutions and the Galerkin least squares method [49] to alleviate instabilities in advection-dominated temperature solutions. For models with a temperature- and stress-dependent rheology, the flow and temperature fields are strongly coupled, and the resulting nonlinear system is efficiently solved using a multicorrector fixed-point algorithm (J. He et al., in preparation, 2004). The resultant linear algebra equation is solved with the commonly used direct LU decomposition method after an optimal node reordering. At each iteration, the flow and temperature fields are solved simultaneously, instead of sequentially. The residuals in velocity and temperature are the maximum difference (the $L_\infty - \text{norm}$) between consecutive iterations, normalized by the maximum value of each. Convergence is achieved with residuals for both velocity and temperature less than 10^{-6}. Little difference in the velocity or temperature field is observed for models that are allowed to converge to 10^{-8}. For models with a nonlinear rheology, 18–20 iterations are required to achieve convergence to 10^{-6}.

We have performed extensive tests to establish the numerical accuracy of our technique (van Keken et al., in preparation, 2004). In particular, we have focussed on the region near the seaward end of the viscous wedge, where the sharp transition from no flow to the full subduction rate introduces mathematical difficulties. By using a high node density in this region and quadratic elements, we are able to accurately model the near-singularity behaviour. Numerical tests show that our method can reproduce the analytic pressure and velocity solutions for an isoviscous wedge [50] to within 0.01% for all parts of the wedge. We have also tested Cascadia models with a landward boundary 500 km from the trench, as used by van Keken et al. [16]. Using their backarc boundary conditions, we are able to reproduce their results for both an isoviscous and nonlinear rheology.

4. Thermal modelling results

4.1. Isoviscous models

We first developed thermal models using a constant mantle wedge viscosity. An isoviscous wedge produces subhorizontal flow in the shallow asthenosphere mantle from the landward boundary toward the corner [8,50]. Fig. 5a shows the modelled thermal structure and heat flow for each of the three landward geotherms. The resultant thermal structure is very sensitive to the prescribed temperatures on the landward boundary.

The most realistic geotherm for the landward boundary of the model is the ‘‘cool’’ geotherm, representative of the adjacent North America craton. With this geotherm, the low temperatures prescribed to the shallow part of this boundary are advected into the wedge, leading to an extremely cold mantle wedge and a nearly constant low heat flow of ~ 40 mW/m^2 across the backarc and at the volcanic arc. For an isoviscous mantle, the flow field is independent of temperature and the absolute value of the viscosity and, thus, flow will occur even when temperatures are extremely low. The ‘‘warm’’ and ‘‘hot’’ landward geotherms produce a hotter wedge, although temperatures are 200–400 °C lower than those inferred from observations. In both cases, the model backarc surface heat flow away from the landward boundary is ~ 60 mW/m^2. In the backarc regions, a seaward decrease in surface heat flow occurs from the prescribed value at the landward boundary. This decrease indicates that the flow velocities in the upper part of the wedge are insufficient to maintain the prescribed initial high geothermal gradient, leading to a conductive cooling of the shallow wedge.

4.2. Nonlinear wedge rheology

A more realistic stress- and temperature-dependent rheology gives a much different flow pattern (Fig. 5b). With this rheology, regions with a high temperature and high strain rate have a low effective viscosity. Due to the nonlinear feedback between the temperature and flow fields, a thin low viscosity channel develops subparallel to the subducting slab. High-velocity flow is concentrated within this channel, resulting in a strong focussing of flow from

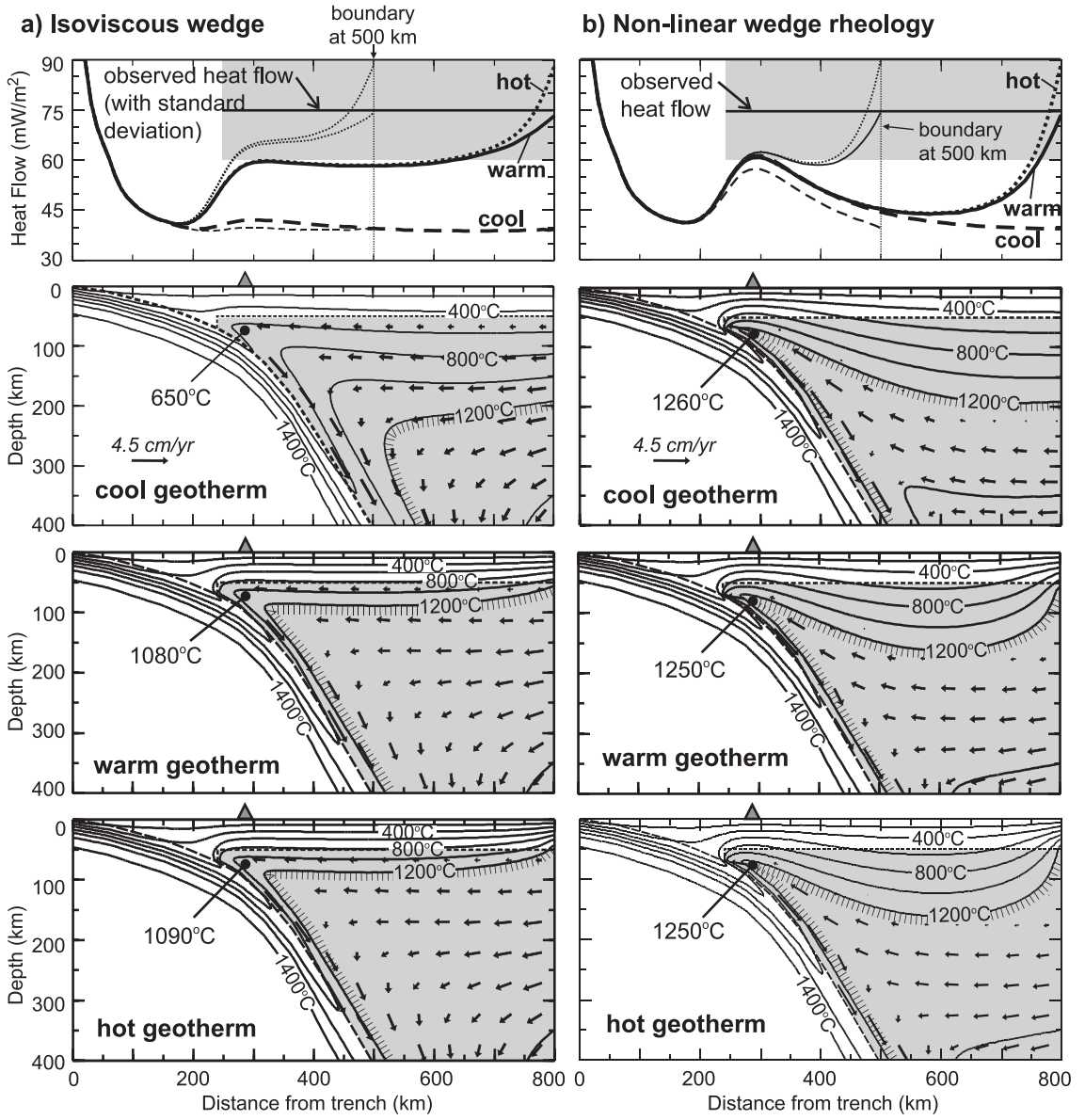

Fig. 5. Cascadia surface heat flow (top) and thermal models (lower three plots) for (a) an isoviscous mantle wedge and (b) a wedge with a nonlinear rheology. The prescribed geotherm on the landward boundary is indicated on each contour plot. The shaded region shows the viscous part of the wedge (where flow was calculated); arrows indicate the calculated flow direction in wedge. Temperature contours are 200 °C. The heat flow is also shown for models with the landward boundary located 500 km from the trench.

depth into the wedge corner, as observed in previous studies that use a nonlinear wedge rheology (e.g., [2,10,11,13,16]). Flow originates at great depths (>150 km) along the backarc boundary, corresponding to the high-temperature part of the prescribed landward geotherm. At these depths, the three geotherms described above have similar temperatures. The similar high temperatures from depth are tapped and rapidly advected upward toward the wedge corner. Therefore, all three geotherms lead to

similar maximum wedge temperatures of 1250–1260 °C below the arc, in fair agreement with the inferred temperature for arc magma generation.

As a direct consequence of the strong flow focussing caused by the nonlinear rheology, a thick, nearly stagnant "lid" develops in the shallow backarc mantle, where feedback between low stresses and low temperatures produces a high viscosity region. Heat is primarily transported by conduction within this lid. For models with "warm" and "hot" landward geotherms, this leads to a cooling of the shallow backarc mantle seaward of the landward model boundary, as reflected by the rapid seaward decrease in surface heat flow (Fig. 5b). Away from the boundary, all three geotherms produce similar wedge temperatures and a backarc heat flow of 40–45 mW/m^2, much lower than observed. Near the volcanic arc, heat flow increases by 15–20 mW/m^2, as flow is focussed upward into the wedge corner. Although the observed heat flow is high near volcanic centres, the regional heat flow does not increase significantly in the area of the volcanic arc [27–29].

The development of the backarc lid is sensitive to the distance between the backarc boundary of the model and the volcanic arc. When this boundary is moved to 200 km from the arc, only a slight cooling is observed in the shallow backarc mantle for the "warm" and "hot" geotherms, due to the proximity of the prescribed high boundary temperatures. Temperatures below the arc are similar to the 800-km models. Most previous modelling studies have placed the backarc boundary fairly close to the volcanic arc [13,15,16]. In studies that use a wide (>600 km) model domain, a similar cool backarc lid is observed (e.g., [2]).

4.3. Mantle potential temperature

Due to the large depth of inflow for the nonlinear viscosity models, the subarc mantle temperatures are most sensitive to the deep (>150 km) temperatures prescribed to the vertical landward boundary, given by the assumed mantle potential (zero pressure) temperature and adiabatic gradient. In the above models, an adiabatic geotherm representing a potential temperature of 1295 °C was used. With a geotherm that represents a potential temperature of 1400 °C (Fig. 4), the maximum mantle temperatures below the volcanic arc are increased by ~ 95 °C, and surface heat flow at the arc is ~ 8 mW/m^2 higher. There is little change in the shallow backarc temperatures or heat flow.

4.4. Rheological parameters

The above models use the rheological parameters for dislocation creep of wet olivine. Reasonable variations in the rheological parameters, including those for dry mantle minerals, have only a small effect on the resulting flow and thermal fields in the wedge. The absolute value of viscosity does not affect the flow structure; it is only the temperature dependence and, to a lesser degree, the stress dependence, that affect the results. With a stronger temperature dependence, flow becomes more focussed into the wedge corner, leading to slightly higher temperatures in the corner and a somewhat cooler backarc. These effects are small, with temperature changes less than 30 °C and heat flow variations less than 3 mW/m^2 for a reasonable range of parameters.

4.5. Variations in subduction parameters and overriding lithosphere thickness

To determine the sensitivity of the models to variations in the subduction geometry, plate age, and subduction rate, we developed models for the contrasting NE Japan subduction zone. This subduction zone has a much older subducting plate (130 Ma), resulting in a cooler incoming plate compared to Cascadia. The subduction rate is 9.1 cm/year, approximately twice that of Cascadia. We use the subducting plate geometry assumed by Peacock and Wang [15]. At depths less than 70 km, the geometry of the plate interface is similar to Cascadia. At greater depths, the plate beneath NE Japan has a dip of 30°, whereas the dip for Cascadia is 60°.

The behaviour of the models is similar to that observed for the Cascadia models for both an isoviscous and a nonlinear wedge rheology. For the isoviscous NE Japan models, temperatures below the volcanic arc are generally >50 °C higher, due to the higher subduction rate and thus wedge flow rate. For a nonlinear wedge rheology, the thermal effects of an increased subduction rate are partially balanced by the shallower plate dip for NE Japan, which limits the maximum depth of inflow, and hence maximum

inflow temperatures, along the backarc boundary of the model. In the backarc, the stagnant lid is slightly thinner, and backarc heat flow and temperatures are slightly higher than for Cascadia, due to the shallower plate dip for NE Japan. Using different combinations of the deep plate geometry, subducting plate age, and subduction rate, we find that these three parameters have only a small effect (< 75 °C) on wedge temperatures below the arc for a given landward geotherm and wedge rheology (Fig. 6).

Variations in the overriding lithosphere thickness do not have a significant effect on the modelled thermal structure. Isoviscous models with a rigid lithosphere as thin as 10 km are slightly cooler (20–50 °C) below the arc, due to more heat loss through the surface. For a nonlinear rheology, the prescribed lithosphere thickness does not affect the results significantly, as the temperature-dependent rheology inhibits flow at shallow depths where there is strong cooling to the surface.

4.6. Thick craton lithosphere at landward boundary

In the above models, flow was allowed to enter the backarc from anywhere along the backarc boundary shallower than the inflow–outflow transition point. We now look at the effects of having a more realistic thick lithosphere along this boundary, which prohibits flow in the wedge from shallow depths (e.g., Fig. 1). Many subduction zones are located adjacent to cratons or stable platforms, including the Cascadia and South America subduction zones. The lithosphere beneath cratons may be 200–400 km thick, based on seismic evidence, surface heat flow, and xenolith thermobarometry [22–24,51,52]. These observations suggest cool temperatures to great depths. The long-term stability of cratonic lithosphere has been attributed to a high viscosity associated with low temperatures, chemical depletion [22,52], and dehydration [53].

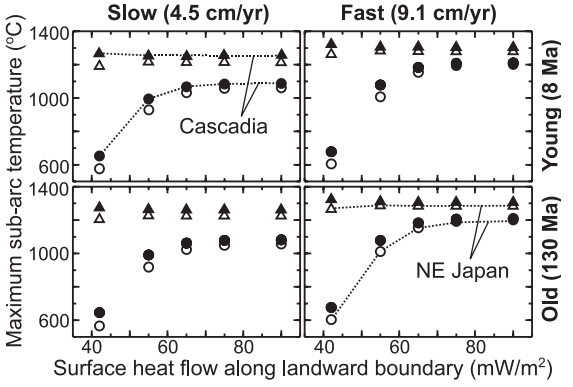

Fig. 6. The maximum mantle wedge temperature beneath the volcanic arc as a function of the prescribed landward geotherm (given by the surface heat flow) for different combinations of subduction rate, subducting plate age, and subducting plate dip (Cascadia geometry: solid symbols; NE Japan geometry: open symbols) for both an isoviscous (circles) and a nonlinear (triangles) mantle rheology.

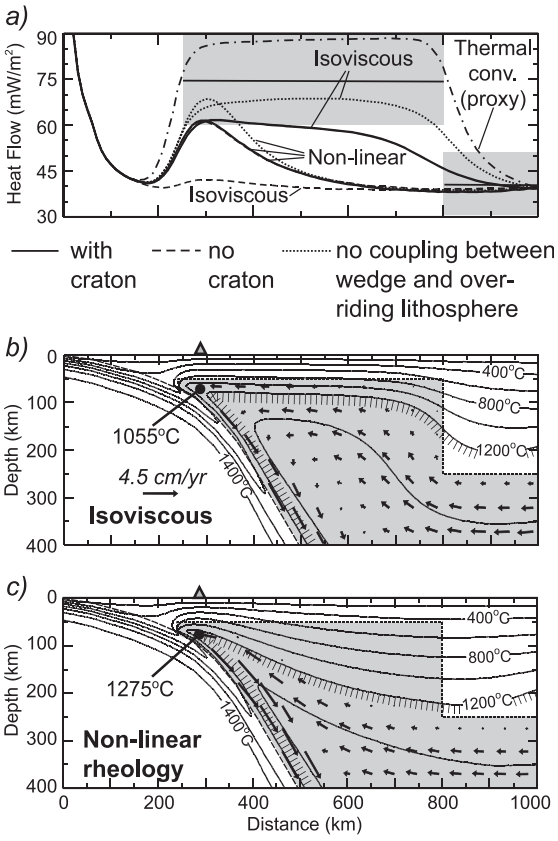

Fig. 7. Cascadia thermal models with a rigid 250-km-thick craton lithosphere located 800 km from the trench. (a) Modelled surface heat flow (see legend). The dot–dashed line is the heat flow for a proxy model in which the effects of extremely vigorous thermal convection ($Nu = 1000$) are simulated. For all models, the cool geotherm was prescribed to the landward boundary of the model. (b) Thermal model cross-section for an isoviscous wedge (200 °C contours). The shaded region indicates where viscous flow was allowed; arrows show flow direction. (c) Same as (b), but for a nonlinear wedge rheology.

To study the effects of thick-craton lithosphere, a rigid rectangular block was introduced to the Cascadia models. The seaward boundary of the block is located 800 km from the trench, consistent with the northern Cascadia backarc width. The block has a thickness of 250 km, similar to estimates of the North America lithosphere thickness from seismic tomography [54–56], xenolith data [51], and thermal arguments [23–25,57]. This thickness also coincides with the transition from a conductive to adiabatic gradient for the "cool" geotherm (Fig. 4).

For an isoviscous mantle wedge, the presence of the thick-craton lithosphere has a significant effect on mantle flow. The rigid craton deflects material from beneath the craton into the mantle wedge, carrying hot material upward, producing a significant heating of the wedge (Fig. 7). Surface heat flow increases from ~ 40 mW/m^2 at the craton to 50–60 mW/m^2 across the backarc. The temperatures below the volcanic arc are ~ 500 °C hotter than models without a craton, although still lower than inferred magma generation temperatures.

For the nonlinear wedge rheology, the presence of a craton has a negligible effect on the thermal structure of the wedge (Fig. 7c), as flow into the wedge already has a deep origin, due to the strong temperature dependence of viscosity. The presence of a craton is not sufficient to alleviate cooling of the backarc produced by the nonlinear rheology.

5. Why is the backarc hot?

Geophysical and geochemical constraints indicate hot (>1200 °C) and nearly isothermal conditions within the upper backarc mantle wedge at subduction zones. Although our study has focussed on the Cascadia subduction zone, a hot backarc appears to be a characteristic of most, if not all, subduction zones; we have not been able to find evidence that any backarc is cool. The heat sink of the cool subducting slab, dehydration reactions, and high backarc heat flow must be balanced by some source of heat.

5.1. Local heat sources in the backarc

There are numerous local heat sources at a subduction zone, but all appear to be insufficient to produce high wedge temperatures. Frictional heating along the top of the slab will primarily affect the forearc region where the subducting slab is in contact with the rigid overriding lithosphere. However, low values of heat flow over the forearc suggest little frictional heating, with estimated shear stresses along the top of the subducting plate of 10–30 MPa (e.g., [7,42]). Viscous dissipation within the mantle wedge depends on both the strain rate and wedge viscosity. For the above models, the strain rate within the wedge is on the order of 10^{-14} s^{-1}. For mantle viscosities less than 10^{20} Pa s, viscous dissipation has only a small effect on the wedge thermal structure (< 50 °C).

Another local heat source may be radiogenic heating in the mantle, through the decay of Th, U, and K isotopes. The mantle wedge may be enriched in radiogenic elements, due to the addition of these elements to the wedge from subducting slab dehydration [14], or through subduction erosion that carries crustal material, high in Th, U, and K, down with the subducting slab [58]. However, mantle xenolith studies suggest that this is a fairly minor heat source (< 0.1 μW/m^3) [14,23]. The fairly low concentration of radiogenic elements in arc magmas that appear to be derived from partial melting in the wedge also argues for low asthenosphere wedge concentrations [14]. In order to have a significant effect on the wedge temperatures, a concentration of radiogenic elements greater than 0.2 μW/m^3 is required. Although no studies have identified such high values in the mantle of backarcs, the magnitude of radiogenic heating within the mantle wedge remains an important uncertainty.

5.2. Assessment of traction-driven mantle wedge flow

Assuming that local heat sources contribute only a small amount to the heat budget, it is necessary to transport heat upward into the wedge by mantle flow. For numerical models of mantle wedge flow driven by a kinematic subducting plate, the thermal structure of the mantle wedge is controlled by the assumed boundary conditions along the backarc boundary, as well as the location of this boundary. For an isoviscous wedge, flow is too slow to transport enough heat into the wedge corner to satisfy constraints on magma generation temperatures, even if unrealistically high temperatures are prescribed to the boundary. By introducing a thick craton lithosphere to the boundary, flow is forced to

originate from depth, elevating temperatures within the wedge, although the temperatures below the arc are still too low for magma generation. With a nonlinear wedge viscosity, flow from depth is focussed into the wedge corner, significantly enhancing temperatures below the arc. While this flow transports enough heat into the wedge corner for magma generation, extremely low backarc temperatures and backarc heat flow are produced. This is clearly inconsistent with the well-constrained thermal structure for the Cascadia backarc and other subduction zones.

The maximum thermal effects of slab-driven wedge flow can be evaluated by considering the maximum wedge flow velocity that can be obtained in a slab-driven flow model. An extreme, although physically unrealistic, model would be to completely decouple the viscous wedge from the overlying lithosphere. For an isoviscous wedge, decoupling leads to a stronger upflow along the seaward craton boundary, and higher flow velocities in the upper backarc mantle. More heat is transported into the wedge, leading to a temperature increase of ~ 100 °C in the shallow backarc, and an increase in heat flow of ~ 10 mW/m^2, barely sufficient to match the observations (Fig. 7a). Beneath the arc, the temperatures are increased by less than 50 °C. For a nonlinear viscosity, decoupling of the lithosphere and asthenosphere only affects the corner region of the wedge. Below the arc, temperatures are increased by 100 °C, and a slightly higher heat flow is produced. The backarc thermal structure is not affected.

In the models, wedge flow was driven by full coupling between the subducting plate and mantle wedge at depths greater than 70 km. Dehydration of the slab as it subducts may produce a thin layer of hydrated mantle material above the slab. Laboratory studies indicate that even a small amount of hydrous fluid can significantly reduce mantle viscosity [59–61]. The low viscosity layer could, to some degree, decouple the slab and mantle wedge, leading to lower flow velocities in the wedge. The addition of hydrous fluids to the mantle may also result in the formation of weak hydrous minerals, such as serpentine [44,62–64]. Both hydration and serpentinization of the mantle immediately above a subducting plate may result in a partial or full decoupling of the slab from the rest of the mantle wedge, leading to slower wedge flow velocities and cooler wedge temperatures than shown above.

These models show that it is not possible to simultaneously produce high temperatures beneath the volcanic arc and backarc using only traction-driven mantle wedge flow. Although the models in this study are steady-state models, they illustrate that subduction is primarily a cooling process. In a time-dependent model, the thermal structure at a given time will depend on the initial conditions prior to subduction, as well as the length of time since subduction started. Over time, the system will evolve toward the steady-state model. Regardless of the time scale, these models are not expected to yield a backarc hotter than the initial conditions.

5.3. Possibility of vigorous thermal convection

In this study, wedge flow driven by thermal buoyancy has been neglected. While the velocity of traction-driven wedge flow is limited by the subduction rate (i.e., a few centimetres per year), thermal convection can produce much more rapid flow. We have not examined such models in detail but can address their overall heat budget. To simulate the thermal effects of vigorous convective flow within the mantle wedge, we use a simple conductive proxy model, following the approach used by Davis et al. [65] and Sharpe and Peltier [66]. In this model, an extremely high thermal conductivity is assigned to the mantle wedge. The ratio of this ‘‘effective’’ thermal conductivity to the true mantle conductivity is equal to the Nusselt number (*Nu*) of the system. This number represents the ratio of the total heat transport to the heat transferred by conduction alone and is therefore a measure of the efficiency of convective heat transfer. Higher *Nu* values indicate more vigorous convection. With a proxy model using an arbitrary Nusselt number of 1000, high temperatures (>1300 °C) are found throughout the wedge and backarc, as reflected by high and constant backarc heat flow (Fig. 7a). Note that the absolute value of heat flow for this model is inversely proportional to the assumed lithosphere thickness, and so the observed heat flow can be matched using this model by varying the lithosphere thickness. The simple proxy model demonstrates the thermal efficiency of vigorous convection, but further thermal convection modelling is required to examine the details.

If thermal convection is important, mantle viscosities at convergent margins must be much lower than

commonly thought, for example, based on postglacial rebound of cratons (e.g., [67]). The viscosity of the wedge may be quite low because it is likely hydrated due to fluid released by dehydration reactions within the subducting plate. In addition, estimated temperatures in the wedge approach the solidus for wet mantle minerals, and thus partial melt may be present, further decreasing the viscosity. Ida [68] suggests that at viscosities less than 10^{20} Pa s, thermal buoyancy may become a significant driving force for mantle wedge flow. Constraints on mantle wedge viscosity from studies of postglacial rebound, postseismic deformation, and dynamic topography suggest a backarc mantle viscosity much less than 10^{20} Pa s, and probably less than 10^{19} Pa s [69–74].

6. Conclusions

Our study provides an evaluation of subduction zone thermal models that include mantle wedge flow driven by a kinematic subducting plate. For these types of models, the location of the backarc model boundary and prescribed conditions along this boundary provide the primary controls on the thermal structure of the wedge. The subducting plate geometry, plate age, and subduction rate have a second-order effect. Given the significant effect that the backarc boundary has on model results, it is important to address the choice of boundary conditions in these models and understand the implications.

The temperatures prescribed to the boundary determine the amount of heat carried into the wedge by flow. The wedge rheology determines the flow pattern, and thus the distribution of heat. For an isoviscous wedge, flow enters the wedge across the backarc boundary at shallow depths, and wedge temperatures are most sensitive to the shallow (<200 km) boundary temperatures. The flow field is fairly diffuse and flow is too slow to carry a significant amount of heat into the wedge corner for arc magma generation, even if extremely high temperatures are prescribed to the backarc boundary. If a thick-craton lithosphere is introduced at the boundary to focus flow from greater depths, temperatures in the backarc are increased, but the arc corner is still too cold for magma generation.

With a stress- and temperature-dependent wedge rheology, the entrained material and return flow are confined to a relatively narrow channel above the subducting plate. In this case, wedge temperatures are determined by the prescribed deep (>150 km) temperatures along the backarc boundary. Flow rapidly carries heat from depth into the wedge corner, significantly enhancing temperatures below the arc. However, if the backarc boundary is located more than 300 km from the arc, a thick, stagnant lid develops in the backarc, leading to low backarc temperatures and heat flow.

Observations of high temperatures and high heat flow for hundreds of kilometres into the backarc provide important constraints for models of mantle wedge dynamics. Traction-driven flow at plate rates transports heat too inefficiently to produce the observed high temperatures throughout the arc and backarc regions. This suggests that an additional component of mantle flow is required. Rapid thermal convection, driven by thermal buoyancy in a low-viscosity mantle wedge, is an effective way to produce a nearly isothermal mantle wedge and backarc and should be examined in future studies.

Acknowledgements

Suggestions by Chris Beaumont, James Conder, Earl Davis, Brad Hacker, Scott King, and an anonymous reviewer greatly improved the manuscript. We thank Peter van Keken for organizing the MARGINS workshop on the thermal structure and dynamics of subduction zones (University of Michigan, October 2002) and the benchmarking exercise for subduction zone thermal models. Support for C.A.C. was provided by an NSERC graduate scholarship (Geological Survey of Canada contribution no. 2003308). ***[SK]***

References

[1] Y. Tatsumi, S. Eggins, Subduction Zone Magmatism, Blackwell, Cambridge, 1995.
[2] P.B. Kelemen, J.L. Rilling, E.M. Parmentier, L. Mehl, B.R. Hacker, Thermal structure due to solid-state flow in the mantle wedge beneath arcs, Am. Geophys. Monogr. 138 (2003) 293–311.
[3] D.P. McKenzie, J.G. Sclater, Heat flow inside the island arcs of the northwestern Pacific, J. Geophys. Res. 73 (1968) 3173–3179.
[4] J.W. Minear, M.N. Toksöz, Thermal regime of a downgoing slab and new global tectonics, J. Geophys. Res. 75 (1970) 1397–1419.

[5] E.R. Oxbugh, D.L. Turcotte, Thermal structure of island arcs, Geol. Soc. Am. Bull. 81 (1970) 1665–1688.
[6] D.A. Yuen, L. Fleitout, G. Schubert, C. Froidevaux, Shear deformation zones along major transform faults and subducting slabs, Geophys. J. R. Astron. Soc. 54 (1978) 91–119.
[7] S.M. Peacock, Thermal and petrologic structure of subduction zones, in: G.E. Bebout, D.W. Choll, S.H. Kirby, J.P. Platt (Eds.), Subduction: Top to Bottom, American Geophysical Union, Washington, DC, 1996, pp. 119–133.
[8] D. McKenzie, Speculations on the consequences and causes of plate motions, Geophys. J. R. Astron. Soc. 18 (1969) 1–32.
[9] N. Sleep, M.N. Toksöz, Evolution of marginal basins, Nature 233 (1971) 548–550.
[10] D.J. Andrews, N.H. Sleep, Numerical modelling of tectonic flow behind island arcs, Geophys. J. R. Astron. Soc. 38 (1974) 237–251.
[11] S. Honda, Thermal structure beneath Tohoku, northeast Japan—a case study for understanding the detailed thermal structure of the subduction zone, Tectonophysics 112 (1985) 69–102.
[12] J.H. Davies, D.J. Stevenson, Physical model of source region of subduction zone volcanics, J. Geophys. Res. 97 (1992) 2037–2070.
[13] Y. Furukawa, Depth of the decoupling plate interface and thermal structure under arcs, J. Geophys. Res. 98 (1993) 20005–20013.
[14] H. Iwamori, Heat sources and melting in subduction zones, J. Geophys. Res. 102 (1997) 14803–14820.
[15] S.M. Peacock, K. Wang, Seismic consequences of warm versus cool subduction metamorphism: examples from southwest and northeast Japan, Science 286 (1999) 937–939.
[16] P.E. van Keken, B. Kiefer, S.M. Peacock, High-resolution models of subduction zones: implications for mineral dehydration and the transport of water into the deep mantle, Geochem. Geophys. Geosyst. 3 (1) (2002) DOI:10.1029/2004GC000256.
[17] J.A. Conder, D.A. Wiens, J. Morris, On the decompression melting structure at volcanic arcs and back-arc spreading centers, Geophys. Res. Lett. 29 (2002) DOI:10.1029/2002GL015390.
[18] R.D. Hyndman, K. Wang, Thermal constraints on the zone of major thrust earthquake failure: the Cascadia subduction zone, J. Geophys. Res. 98 (1993) 2039–2060.
[19] R.D. Hyndman, T.J. Lewis, Geophysical consequences of the Cordillera–Craton thermal transition in southern Canada, Tectonophysics 306 (1999) 397–422.
[20] E.E. Davis, T.J. Lewis, Heat flow in a back-arc environment: Intermontane and Omineca crystalline belts, southern Canadian Cordillera, Can. J. Earth Sci. 21 (1984) 715–726.
[21] H. Gabrielse, Structural styles, Chapter 17 (Comp.), in: H. Gabrielse, C.J. Yorath (Eds.), Geology of the Cordilleran Orogen in Canada, Geology of Canada, vol. 4, Geological Survey of America, Boulder, CO, 1991, pp. 571–675.
[22] T.H. Jordan, The continental tectosphere, Rev. Geophys. Space Phys. 13 (1975) 1–13.
[23] R.L Rudnick, W.F. McDonough, R.J. O'Connell, Thermal structure, thickness and composition of continental lithosphere, Chem. Geol. 145 (1998) 395–411.
[24] C. Jaupart, J.C. Mareschal, The thermal structure and thickness of continental roots, Lithos 48 (1999) 93–114.
[25] I.M. Artemieva, W.D. Mooney, Thermal thickness and evolution of Precambrian lithosphere: a global study, J. Geophys. Res. 106 (2001) 16387–16414.
[26] T.J. Lewis, W.H. Bentkowski, E.E. Davis, R.D. Hyndman, J.G. Souther, J.A. Wright, Subduction of the Juan de Fuca plate: thermal consequences, J. Geophys. Res. 93 (1988) 15207–15225.
[27] D.D. Blackwell, J.L. Steele, S. Kelley, M.A. Korosec, Heat flow in the state of Washington and thermal conditions in the Cascade range, J. Geophys. Res. 95 (1990) 19495–19516.
[28] D.D. Blackwell, J.L. Steele, M.K. Frohme, C.F. Murphey, G.R. Priest, G.L. Black, Heat flow in the Oregon Cascade Range and its correlation with regional gravity, curie point depths, and geology, J. Geophys. Res. 95 (1990) 19475–19493.
[29] T.J. Lewis, W.H. Bentkowski, R.D. Hyndman, Crustal temperatures near the Lithoprobe Southern Canadian Cordillera Transect, Can. J. Earth Sci. 29 (1992) 1197–1214.
[30] R.D. Hyndman, The Lithoprobe corridor across the Vancouver Island continental margin: the structural and tectonic consequences of subduction, Can. J. Earth Sci. 32 (1995) 1802–1977.
[31] L.T. Elkins Tonaton, T.L. Grove, J. Donnelly-Nolan, Hot, shallow melting under the Cascades volcanic arc, Geology 29 (2001) 631–634.
[32] M. Springer, A. Forster, Heat-flow density across the central Andean subduction zone, Tectonophysics 291 (1998) 123–129.
[33] A.Y. Babeyko, S.V. Sobolev, R.B. Trumbull, O. Oncken, L.L. Lavier, Numerical models of crustal scale convection and partial melting beneath the Altiplano-Puna plateau, Earth Planet. Sci. Lett. 1999 (2002) 373–388.
[34] T. Wanatabe, M.G. Langseth, R.N. Anderson, Heat flow in back-arc basins of the western Pacific, in: M. Talwani, W.C. Pittman III (Eds.), Island Arcs, Deep Sea Trenches and Back-Arc Basins, Maurice Ewing Series 1, American Geophysical Union, Washington, DC, 1977, pp. 137–161.
[35] P. Flück, R.D. Hyndman, K. Wang, 3-D dislocation model for great earthquakes of the Cascadia subduction zone, J. Geophys. Res. 102 (1997) 20539–20550.
[36] M.G. Bostock, J.C. van Decar, Upper mantle structure of the northern Cascadia subduction zone, Can. J. Earth Sci. 32 (1995) 1–12.
[37] R.M. Clowes, C.A. Zelt, J.R. Amor, R.M. Ellis, Lithospheric structure in the southern Canadian Cordillera from a network of seismic refraction lines, Can. J. Earth Sci. 32 (1995) 1485–1513.
[38] M.J.A. Burianyk, E.R. Kanasewich, N. Udey, Broadside wide-angle seismic studies and three-dimensional structure of the crust in the southeast Canadian Cordillera, Can. J. Earth Sci. 34 (1997) 1156–1166.
[39] J.V. Ross, The nature and rheology of the Cordilleran upper mantle of British Columbia: inferences from peridotite xenoliths, Tectonophysics 100 (1983) 321–357.

[40] S. Karato, P. Wu, Rheology of the upper mantle: a synthesis, Science 260 (1993) 771–778.
[41] S. Mazzotti, H. Dragert, J. Henton, M. Schmidt, R. Hyndman, T. James, Y. Lu, M. Craymer, Current tectonics of northern Cascadia from a decade of GPS measurements, J. Geophys. Res. 108 (2003) DOI:10.1029/2003JB002653.
[42] K. Wang, T. Mulder, G.C. Rogers, R.D. Hyndman, Case for very low coupling stress on the Cascadia subduction fault, J. Geophys. Res. 100 (1995) 12907–12918.
[43] M.G. Bostock, R.D. Hyndman, S. Rondenay, S.M. Peacock, An inverted continental Moho and serpentinization of the forearc mantle, Nature 417 (2002) 536–538.
[44] R.D. Hyndman, S.M. Peacock, Serpentinization of the forearc mantle, Earth Planet. Sci. Lett. 212 (2003) 417–432.
[45] C. Clauser, E. Huenges, Thermal conductivity of rocks and minerals, in: T. Ahrens (Ed.), Rock Physics and Phase Relations: A handbook of Physical Constants, American Geophysical Union, Washington, 1995, pp. 105–126.
[46] C.A. Stein, S. Stein, A model for the global variation in oceanic depth and heat-flow with lithospheric age, Nature 359 (1992) 123–129.
[47] K. Wang, E.E. Davis, Thermal effect of marine sedimentation in hydrothermal active areas, Geophys. J. Int. 110 (1992) 70–78.
[48] E. Ito, T. Katsura, A temperature profile of the mantle transition zone, Geophys. Res. Lett. 16 (1989) 425–428.
[49] T.J.R. Hughes, L.P. Franca, G.M. Hulbert, A new finite element formulation for computational fluid dynamics: VIII. The Galerkin-Least-Squares method for advective–diffusive equations, Comput. Methods Appl. Mech. Eng. 73 (1989) 173–189.
[50] G.K. Batchelor, An Introduction to Fluid Dynamics, Cambridge Univ. Press, New York, 1967, 615 pp.
[51] J.K. Russell, M.G. Kopylova, A steady state conductive geotherm for the north central Slave, Canada: inversion of petrological data from the Jericho Kimberlite pipe, J. Geophys. Res. 104 (1999) 7089–7101.
[52] A.M. Forte, H.K.C. Perry, Geodynamic evidence for a chemically depleted continental tectosphere, Science 290 (2000) 1940–1944.
[53] G. Hirth, R.L. Evans, A.D. Chave, Comparison of continental and oceanic mantle electrical conductivity: is the Archean lithosphere dry? Geochem. Geophys. Geosyst. 1 (2000) DOI:2000GC000048.
[54] S.P. Grand, Mantle shear structure beneath the Americas and surrounding oceans, J. Geophys. Res. 99 (1994) 11591–11621.
[55] S. van der Lee, G. Nolet, Upper mantle S velocity structure of North America, J. Geophys. Res. 102 (1997) 22815–22838.
[56] A.W. Frederiksen, M.G. Bostock, J.F. Cassidy, S-wave velocity structure of the Canadian upper mantle, Phys. Earth Planet. Inter. 124 (2001) 175–191.
[57] C. Jaupart, J.C. Mareschal, L. Guillou-Frottier, A. Davaille, Heat flow and thickness of the lithosphere in the Canadian Shield, J. Geophys. Res. 103 (1998) 15269–15286.
[58] D.W. Scholl, R. von Huene, Evidence for, and amounts of, continental crustal material recycled to the mantle at Cenozoic subduction zones, Abstracts with Program, 2003 Annual Meeting of the Geological Society of America, GSA (2003).
[59] G. Hirth, D.L. Kohlstedt, Water in the oceanic upper mantle: implications for rheology, melt extraction and the evolution of the lithosphere, Earth Planet. Sci. Lett. 144 (1996) 93–108.
[60] S. Mei, D.L. Kohlstedt, Influence of water on plastic deformation of olivine aggregates: 1. Diffusion creep regime, J. Geophys. Res. 105 (2000) 21457–21469.
[61] S. Mei, D.L. Kohlstedt, Influence of water on plastic deformation of olivine aggregates: 2. Dislocation creep regime, J. Geophys. Res. 105 (2000) 21471–21481.
[62] S.M. Peacock, Fluid processes in subduction zones, Science 248 (1990) 329–337.
[63] P. Ulmer, V. Trommsdorff, Serpentine stability to mantle depths and subduction-related magmatism, Science 268 (1995) 858–861.
[64] S.M. Peacock, R.D. Hyndman, Hydrous minerals in the mantle wedge and the maximum depth of subduction thrust earthquakes, Geophys. Res. Lett. 26 (1999) 2517–2520.
[65] E.E. Davis, K. Wang, J. He, D.S. Chapman, H. Villinger, A. Rosenberger, An unequivocal case for high Nusselt number hydrothermal convection in sediment-buried igneous oceanic crust, Earth Planet. Sci. Lett. 146 (1996) 137–150.
[66] H.N. Sharpe, W.R. Peltier, A thermal history for the Earth with parameterized convection, Geophys. J. R. Astron. Soc. 59 (1979) 171–203.
[67] J.X. Mitrovica, W.R. Peltier, Constraints on mantle viscosity based upon the inversion of post-glacial uplift data from the Hudson Bay region, Geophys. J. Int. 122 (1995) 353–377.
[68] Y. Ida, Convection in the mantle wedge above the slab and tectonic processes in subduction zones, J. Geophys. Res. 88 (1983) 7449–7456.
[69] M.I. Billen, M. Gurnis, A low viscosity wedge in subduction zones, Earth Planet. Sci. Lett. 193 (2001) 227–236.
[70] T.S. James, J.J. Clague, K. Wang, I. Hutchinson, Postglacial rebound at the northern Cascadia subduction zone, Quat. Sci. Rev. 19 (2000) 1527–1541.
[71] G. Khazaradze, K. Wang, J. Klotz, Y. Hu, J. He, Prolonged post-seismic deformation of the 1960 great Chile earthquake and implications for mantle rheology, Geophys. Res. Lett. 22 (2002) DOI:10.1029/2002GL015986.
[72] T. Nishimura, W. Thatcher, Rheology of the lithosphere inferred from postseismic uplift following the 1959 Hebgen Lake earthquake, J. Geophys. Res. 108 (2003) DOI:10.1029/2002JB002191.
[73] H. Ueda, M. Ohtake, H. Sato, Postseismic crustal deformation following the 1993 Hokkaido Nansei-oki earthquake, northern Japan: evidence for a low-viscosity zone in the uppermost mantle, J. Geophys. Res. 108 (2003) DOI:10.1029/2002JB002067.
[74] M. Vergnolle, R. Pollitz, E. Calais, Constraints on the viscosity of the continental crust and mantle from GPS measurements and postseismic deformation models in western Mongolia, J. Geophys. Res. 108 (2003) DOI:10.1029/2002JB002374.